DESIGN OF A μ SYNTHESIS CONTROLLER TO STABILIZE AN UNMANNED HELICOPTER

Wei Yuan[*] , Jay Katupitiya[*]
[*]**School of Mechanical and Manufacturing Engineering, The University of New South Wales, Sydney**
w.yuan@unsw.edu.au; J.Katupitiya@unsw.edu.au

Keywords: *centralized controller, μ synthesis, stabilizing control, unmanned helicopters*

Abstract

This paper presents the design of a centralized controller via μ synthesis for an unmanned helicopter. It is well known that partitioned controllers for a helicopter are based on partitioned systems and usually are in multi-loop manner. When the system is subjected to internal and external disturbances, the tuning of such a control system is very difficult and time-consuming. In this work, the centralized μ-controller (i.e. the controller designed using the un-partitioned helicopter system) for velocity and heading rate control is designed while a substantial amount of sensor noises, external disturbances in the form of wind gusts and model uncertainties is taken into account. The controller is then tested in simulations and briefly compared with a variant of H_∞ controller.

1 Introduction

The R&D into UAVs have achieved significant progresses in the last few decades. Among these, scale-model helicopters are particularly attractive as they are capable of various useful maneuvering modes such as hovering, vertical takeoff-landing, low-speed cruise, pirouette, etc. There are fundamentally two distinct domains to use scale model helicopters, i.e. quasi-steady tracking and aggressive maneuvering. Since our interest is to develop a highly reliable navigation platform, the control problem in hover and low-speed flight, where the most meaningful applications, such as navigation and surveillance, are carried out, is the focus.

But helicopters are naturally unstable, nonlinear and highly coupled. Fortunately, the helicopter dynamics in hover and low-speed flight is mostly linear and can be considered as a LTI MIMO system. In our previous work [1, 2], LTI MIMO state space models were successfully used in system identification to extract the hover dynamics from flight data. Peng and Cai *et al.* [3] applied an identified LTI MIMO helicopter model to realize a near-hover autonomous flight which consisted of tasks including automatic takeoff & landing, hovering, slithering, pirouetting and spiral turning, etc.

One of the core challenges of designing a control system for near-hover flight is to stabilize the vehicle at the working point. For that, various control techniques, such as classical PID [4, 5], Model Predictive Control [6], H_∞ control [7], μ-synthesis [8], Composite Nonlinear Feedback (CNF) method [3] and Neutral Network method [9], have been presented in the literature. However, many of them are in decentralized forms, i.e., the control laws are implemented to partitioned subsystems separately and the entire control systems have multi-loops. Totally, several controllers have to be designed in multi-loops to realize the position and heading control. In order to satisfy multiple requirements for different channels simultaneously, the tuning of all these controllers would be difficult and time-consuming. Besides, the coupling effects in a helicopter among different channels, basically longitudinal dynamics, lateral dynamics, heave dynamics and yaw dynamics, are its nature and cannot be ignored [10]. The decentralized controllers are not much competent to take the coupling effects into account. Therefore, a controller in a centralized manner would be better suited to this scenario.

Looking deeper into the system, the stabilizing control of the directional velocities and the heading rate in the presence of sensor noise and external disturbance and unmodeled dynamics would be the primary task to be solved. After the platform has been stabilized at this level, a further position and heading control would be very easy. La Civita *et al.* [11] presented an autonomous navigation control system for a robotic helicopter. A multi-loop controller based on H_∞ loop shaping method was used to stabilize the three directional velocities v_x, v_y, v_z and the heading rate $\dot{\Psi}$. Instead, Cai *et al.* applied a single-loop H_∞ static output-feedback control to stabilize the velocities and heading rate using only one loop [12]. It makes the stabilizing problem much easier to tune. But this method, as well as the H_∞ loop shaping method can only achieve a general robust performance by shaping the open loop model with pre- and post-compensators (W_1 and W_2) [11, 13, 14]. They would become less attractive when more information about internal and external disturbances needs to be taken into account and multi requirements are to be satisfied in the control design.

In order to cope with noise attenuation, disturbance rejection and model uncertainty in a coupled system as explicitly as possible, the μ-synthesis control method [15] provides great potential to design such a robust centralized controller to stabilize a helicopter.

The objective of our work is to design a centralized controller to stabilize three directional velocities and yaw rate in a single loop using the μ-synthesis. The performance of the controller in non-aggressive autonomous flights is tested in simulations against simulated external wind gusts, sensor noises and system uncertainties. A widely published linearized Yamaha R-50 helicopter model [8] is used in the simulations as the "true" platform which is trimmed and flies with a quasi-constant rotor speed of 900 RPM in hover and near hover condition. Although the model simplifies the real situation, it describes the dynamics in hover and near hover condition well [16].

2 Simulation Platform

2.1 Hover Model

As mentioned above, the scale-model helicopter is a nonlinear, naturally unstable, highly coupled and multiple-input-multiple-output system, but the dynamics in hover and near hover condition can be linearized as a LTI MIMO state space model at the trimmed point. The model is called as hover model here for short. The model structure used in this paper is based on Mettler's work on the identification of helicopter models [10, 16]. The linearized hover model is given by,

$$\dot{x} = Ax + Bu \quad \text{and} \tag{1}$$

$$y = Cx, \tag{2}$$

where $x = [u\ v\ p\ q\ \Phi\ \Theta\ a\ b\ w\ r\ r_{fb}]^T$ is the state vector with u, v, w as the longitudinal, lateral and vertical velocities, respectively; p, q, r are the roll, pitch and yaw rates, respectively; a, b as the longitudinal and lateral flapping angles, respectively with Φ and Θ as roll and pitch angles, respectively. The stick input is $u = [\delta_{lat}\ \delta_{lon}\ \delta_{col}\ \delta_{ped}]^T$ where the elements in the order are: roll rate control, pitch rate control, collective pitch control and the yaw rate control. The output vector is, $y = [u\ v\ w\ p\ q\ r\ \Phi\ \Theta]^T$. The matrices A and B in Eq. 1 are:

$$A = \begin{bmatrix} X_u & 0 & 0 & 0 & 0 & -g & -g & 0 & 0 & 0 & 0 \\ 0 & Y_v & 0 & 0 & g & 0 & 0 & g & 0 & 0 & 0 \\ L_u & L_v & 0 & 0 & 0 & 0 & L_a & L_b & 0 & 0 & 0 \\ M_u & M_v & 0 & 0 & 0 & 0 & M_a & M_b & 0 & 0 & 0 \\ 0 & 0 & 1 & 0 & 0 & 0 & 0 & 0 & 0 & 0 & 0 \\ 0 & 0 & 0 & 1 & 0 & 0 & 0 & 0 & 0 & 0 & 0 \\ 0 & 0 & 0 & -1 & 0 & 0 & \frac{-1}{\tau_a} & A_b & 0 & 0 & 0 \\ 0 & 0 & -1 & 0 & 0 & 0 & B_a & \frac{-1}{\tau_a} & 0 & 0 & 0 \\ 0 & 0 & 0 & 0 & 0 & 0 & Z_a & Z_b & Z_w & Z_r & 0 \\ 0 & 0 & N_p & 0 & 0 & 0 & 0 & 0 & N_w & N_r & N_{rf} \\ 0 & 0 & 0 & 0 & 0 & 0 & 0 & 0 & 0 & K_r & K_{rf} \end{bmatrix} \tag{3}$$

$$B = \begin{bmatrix} 0 & 0 & 0 & 0 \\ 0 & 0 & 0 & 0 \\ 0 & 0 & 0 & 0 \\ 0 & 0 & 0 & 0 \\ 0 & 0 & 0 & 0 \\ 0 & 0 & 0 & 0 \\ A_{lat} & A_{lon} & 0 & 0 \\ B_{lat} & B_{lon} & 0 & 0 \\ 0 & 0 & Z_{col} & 0 \\ 0 & 0 & N_{col} & N_{ped} \\ 0 & 0 & 0 & 0 \end{bmatrix} \tag{4}$$

2.2 Measurement Noises

In the real-life situation, the onboard IMU has build-in observers that can provide high accurate estimation of local velocities and angles, u, v,w, r, Φ and Θ. These signals are very reliable and don't contain much noise, so instead of using the raw measurements that are the angular and linear accelerations, u, v,w, r, Φ and Θ are taken as feedback in the control design. Considerable noises (see Fig. 1) are added to corrupt each of the feedback signals.

2.3 External Disturbances

The external disturbances can be assumed as gust velocity components that perturb the helicopter's directional velocity states u, v and w [13]. The disturbance model used in this work is shown in Fig.2 which represents strong wind gust compared to helicopter's velocities. The wind gusts in x and y directions are assumed to be the same

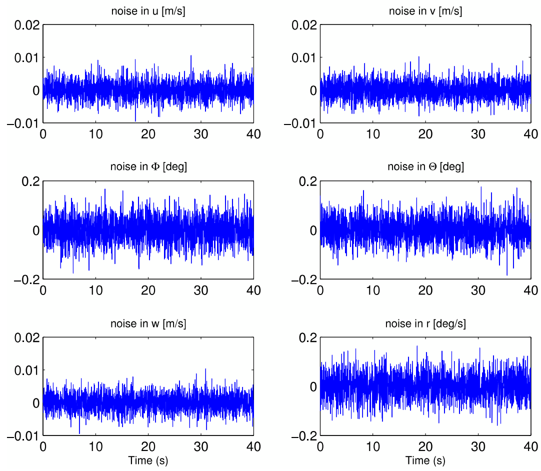

Fig. 1 Measurement Noises.

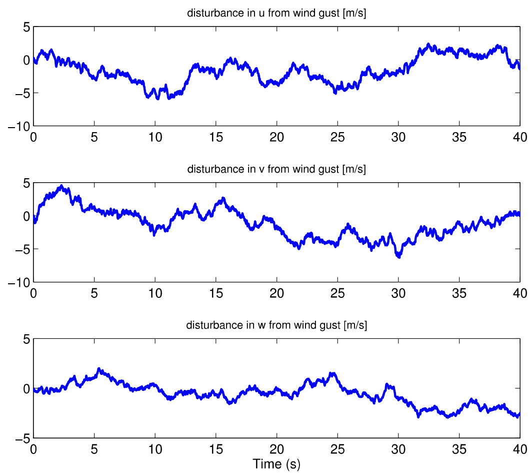

Fig. 2 External Disturbances.

level and the vertical wind gust is a little weaker than them.

3 Controller Design

3.1 μ-synthesis Controller

The μ-synthesis method is very effective for multi-variable robust control problems in which the control system must take several objectives into account simultaneously [13, 15]. Before applying μ-synthesis to find a stabilizing controller, the system specification including the information about measurement noises, external disturbances, model uncertainties and desired performance etc., should be specified and interpreted

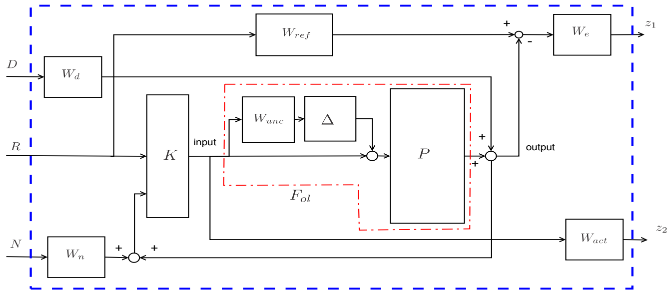

Fig. 3 The μ-synthesis control design

using frequency-domain weighting functions to describe the frequency characteristics of the system specification. The μ-synthesis robust control design problem with weighted performance was shown in Fig. 3.

Compared to the robust control methods that are based on H_∞ method, μ-synthesis is able to take the measurement noise N, the external disturbance D and the model uncertainty Δ into account when designing and synthesizing the controller K.

The plant of the open-loop system F_{ol} includes the nominal model P and the multiplicative uncertainty model $\Delta\mathbf{W}_{unc}$ that is used to lump modelling errors as the uncertainty model at the input. Δ represents the complex structured uncertain dynamics

$$\Delta = \{diag(\Delta_1, \Delta_2, \Delta_3, \Delta_4), \| \Delta_i \|_\infty \leq 1, i = 1,..,4\} \tag{5}$$

As the helicopter has four inputs, a single Δ_i is added to each input. The Δ_i is in the form of a stable first-order transfer function and the values of its coefficients are unknown but $\| \Delta_i \|_\infty \leq 1$.

The weighting function $\mathbf{W}_{unc}$ specifies the uncertainty over the frequency [17]. The small uncertainty $\mathbf{W}_{unc1}$ (case 1 in Fig. 4) means that the helicopter model (Eq. 1) is appropriate to capture the real helicopter dynamics well in the low frequency range between 0.1 to 20 rad/s [10]. The model accuracy drops with increasing frequency. Besides that, we assume that certain error of 10% exists between the model and real plant in the low frequency range. $\mathbf{W}_{unc1}$ is put into μ-synthesis control design procedure to let

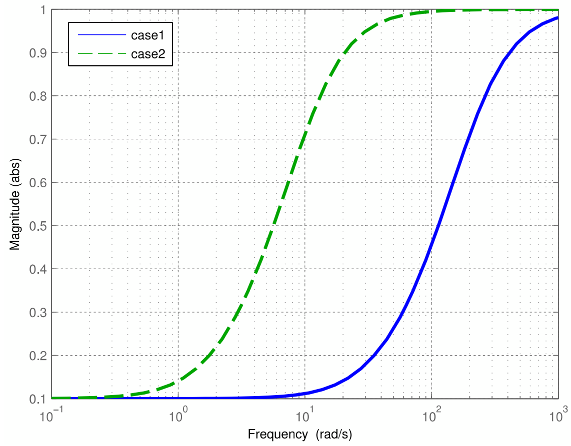

Fig. 4 Uncertainty Model.

the μ-synthesis take the model uncertainty into account.

$$\mathbf{W}_{unc1} = diag\{W_{unc1,1}, W_{unc1,2}, W_{unc1,3}, W_{unc1,4}\} \tag{6}$$

where $W_{unc1,i} = \frac{s+20}{s+200}$, i=1,2,3,4.

The large uncertainty $\mathbf{W}_{unc2}$ (case 2 in Fig. 4) represents that the model is inaccurate even at low frequencies, the uncertainty increases significantly from about 2 rad/s. This large uncertainty will be added to the plant to test the robust performance of the controller in the simulation test section.

$$\mathbf{W}_{unc2} = diag\{W_{unc2,1}, W_{unc2,2}, W_{unc2,3}, W_{unc2,4}\} \tag{7}$$

where $W_{unc2,i} = \frac{0.1(s+1)}{0.1s+1}$, i=1,2,3,4.

$\mathbf{W}_{ref}$ represents the desired model for the closed-loop system. We force u, v and w to follow the same second-order model response, Φ and Θ to have a slightly quicker response and r to response a little much quicker than all other outputs (Fig.5).

$$\mathbf{W}_{ref} = diag\{W_u, W_v, W_w, W_\Phi, W_\Theta, W_r\} \tag{8}$$

where,

$$W_u = W_v = W_w = \frac{\omega_1^2}{s^2 + 2\omega_1 + \omega_1^2}, \ \omega_1 = 0.8\pi,$$

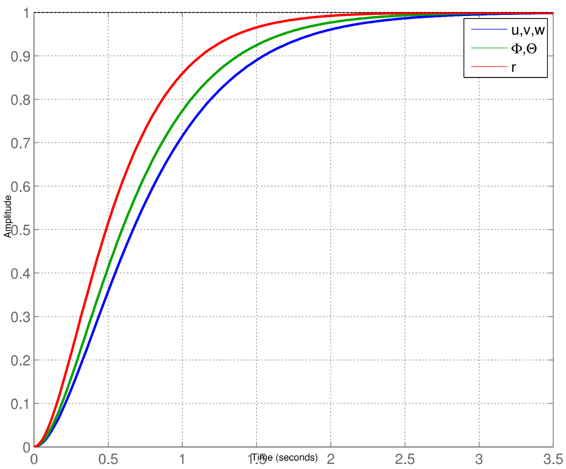

Fig. 5 The step responses of the desired model

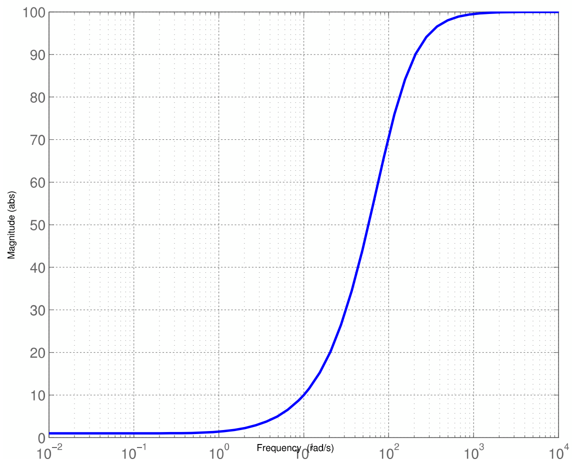

Fig. 6 The actuator penalty function

$W_\Phi = W_\Theta = \dfrac{\omega_2^2}{s^2 + 2\omega_2 + \omega_2^2}$, $\omega_2 = 0.9\pi$ and

$W_r = \dfrac{\omega_3^2}{s^2 + 2\omega_3 + \omega_3^2}$, $\omega_3 = 1.1\pi$.

$\mathbf{W}_d$ describes the frequency characteristics of the external disturbances showing in Fig. 2. The model is based on the wind gust disturbance model shown in Skogestad *et al*[13] and is equal to a strong wind compared to the hover and low-speed flight (Fig. 11):

$$\mathbf{W}_d = diag\left\{W_{dx}, W_{dy}, W_{dz}\right\} \quad (9)$$

where $W_{dx} = W_{dy} = 200\frac{0.15}{s+0.15}$ and $W_{dz} = 100\frac{0.15}{s+0.15}$.

$\mathbf{W}_n$ represents the frequency domain model of the noise in the feedback signals. Each noise singal shown in Fig. 1 has one model. As the feedback signals are estimated by the build-in Observer in IMU, the noise level is very low:

$$\mathbf{W}_n = diag\left\{W_{nu}, W_{nv}, W_{n\Phi}, W_{n\Theta}, W_{nw}, W_{nr}\right\} \quad (10)$$

where $W_{nu} = W_{nv} = W_{nw} = 0.006\dfrac{\frac{1}{70}s+1}{\frac{1}{100}s+1}$ and $W_{n\Phi} = W_{n\Theta} = W_{nr} = 0.0006\dfrac{\frac{1}{70}s+1}{\frac{1}{100}s+1}$.

W_{act} is to shape the penalty on the control signal usage to limit input magnitudes at high frequencies due to the dynamic limits of the actuators. The same first-order high-pass filter (Fig.6) is used in each input channel to penalize the control action at higher than 20 rad/s .

$$\mathbf{W}_{act} = diag\left\{W_{act,1}, W_{act,2}, W_{act,3}, W_{act,4}\right\}. \quad (11)$$

where $W_{act,i} = \dfrac{s+1}{\frac{1}{100}s+1}$, $i = 1,2,3,4$.

$\mathbf{W_e}$ weighs the performance of the closed-loop system compared with the ideal response. The difference between u_{ref} and u, v_{ref} and v, w_{ref} and w and also r_{ref} and r are weighted. We tuned the W_e according to the suggestion in [17], that is, W_e is flat at low frequency, rolls off at first or second order, and flattens out at a small, nonzero value at high frequency. In this way, the response accuracy of the closed model at low frequencies is weighted. The same weighting function (Fig. 7) is applied to each error.

$$\mathbf{W}_e = diag\left\{W_{e,1}, W_{e,2}, W_{e,3}, W_{e,4}\right\}. \quad (12)$$

where $W_{e,i} = \dfrac{s+1}{\frac{1}{100}s+1}$, $i = 1,2,3,4$.

Under the framework (Fig. 3), the input vector of the weighted closed-loop system is $\mathbf{w} = [D\ R\ N]^T$ and the system output vector is $\mathbf{z} = [z_1\ z_2]^T$. Taking $T(P,K)$ as the closed-loop MIMO mapping from $[D\ R\ N]^T$ to $[z_1\ z_2]^T$

$$\mathbf{z} = \mathbf{T}(\mathbf{P},\mathbf{K})\mathbf{w} \quad (13)$$

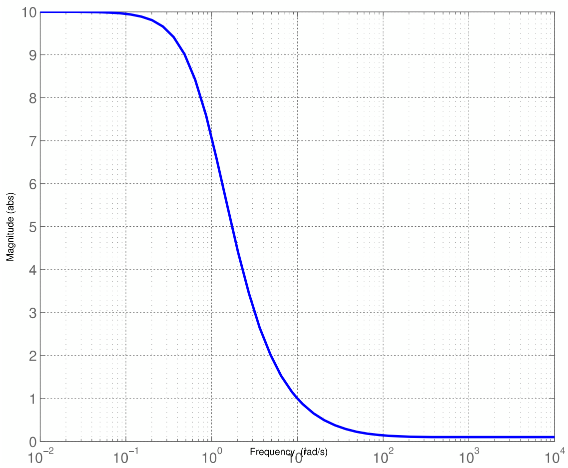

Fig. 7 The performance weighting

the mathematical objective of the control design is to to find an stabilizing controller K, such that for all perturbations $\Delta_{pert} \in \widetilde{\Delta}$, $\| \Delta_{pert} \|_\infty \leq 1$, the closed-loop system T is stable and satisfies

$$\| T[F_{ol}(P, \Delta_{pert}), K] \|_\infty \leq 1. \qquad (14)$$

The control problem above can be recasted into the general μ problem diagram (Fig.8), the goal of μ-synthesis is to minimize the singular value $\mu_{\Delta_{pert}}(.)$ of the closed-loop transfer function T for all perturbations $\Delta_{pert} \in \widetilde{\Delta}$ over all stabilizing controllers K [17], i.e.,

$$\min_K \max_\omega \mu_{\Delta_{pert}}[T(j\omega)] \qquad (15)$$

The augmented block structure $\widetilde{\Delta}$ has the following form:

$$\widetilde{\Delta} = \left\{ \begin{bmatrix} \Delta & 0 \\ 0 & \Delta_P \end{bmatrix} : \Delta \in C^{4\times 4}, \Delta_P \in C^{n_w \times n_z} \right\} \qquad (16)$$

where Δ_P is a fictitious uncertainty block which is used in μ-synthesis to assess the robust performance[15]. It connects **w** and **z** with dimension $n_w \times n_z$.

The implementation of the μ-synthesis controllers were carried out using MATLAB® Robust Control Toolbox.

4 Results

With the proposed centralized stabilizing controller, the closed-loop system provides a simple

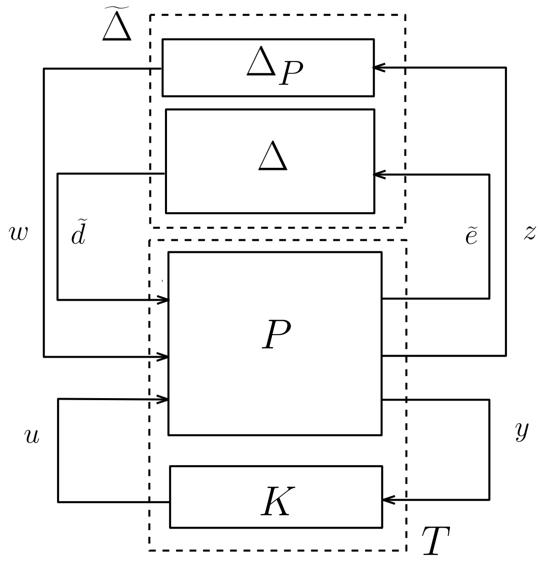

Fig. 8 Description of the μ-synthesis problem

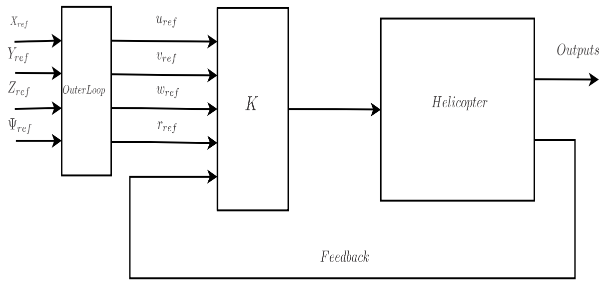

Fig. 9 The two-loop control structure

interface (Fig. 9) for the next control level, position and heading control. A simple path planning layer is added as the outer loop here to generate velocity commands u_{ref}, v_{ref}, w_{ref} and r_{ref} from position and heading commands via the smoothed differential function f (Eq. 17) in each channel.

$$f = \frac{\omega_{n1}^2 s}{s^2 + 2\omega_{n1} + \omega_{n1}^2}, \omega_{n1} = 0.4\pi \qquad (17)$$

For the comparison purpose, another centralized controller based on the signal-based H_∞ method [13] is presented here along with the μ-controller.

The first test (Test 1) is carried out with the small model uncertainty (case 1 in Fig. 4). The measurement noises (Fig. 1) and the windgust disturbances (Fig. 2) are added in the simula-

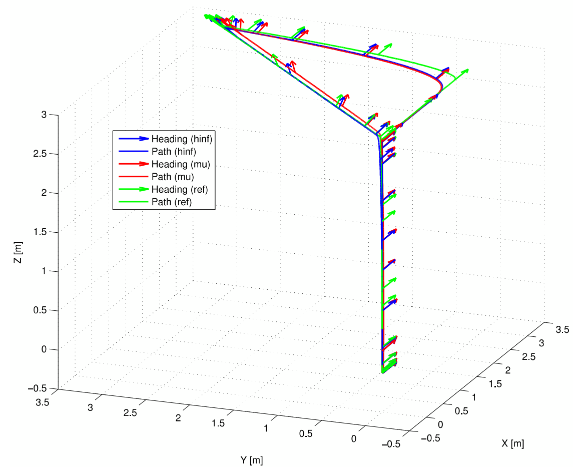

Fig. 10 Test 1-Simple flight path.

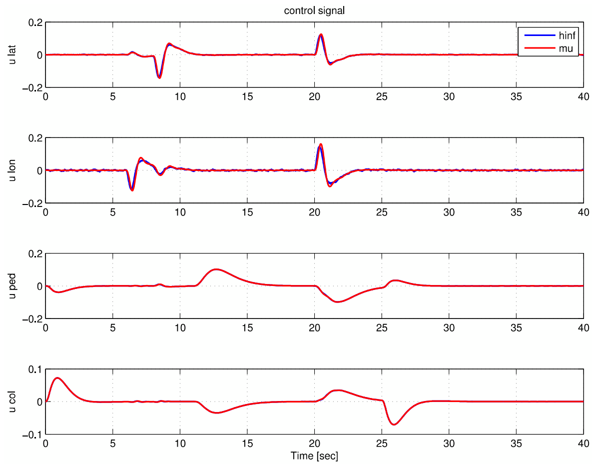

Fig. 13 Test 1 - Inputs to the four actuators.

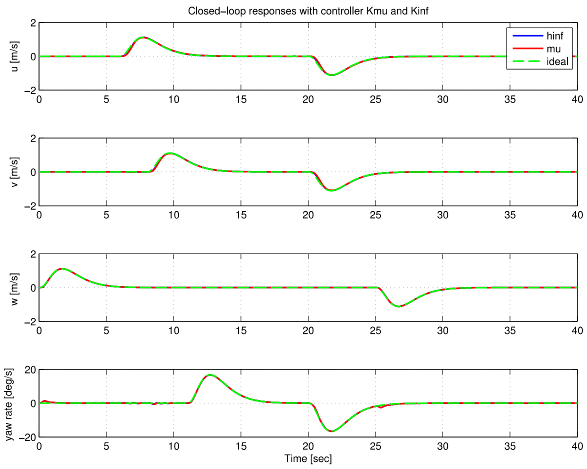

Fig. 11 Test 1 - Controlled velocities.

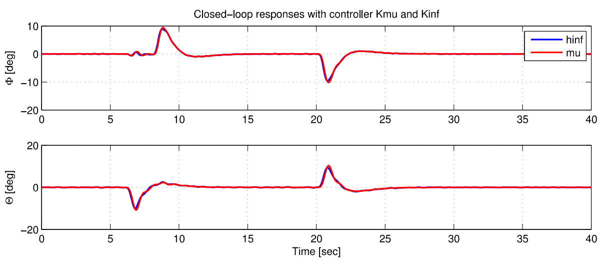

Fig. 12 Test 1 - Controlled roll and pitch.

tions. The simulation results of the controllers are shown in Fig. 10.

In Test 2, the model uncertainty, case 2 (Fig. 4), is added and other parameters, noises and disturbances keep unchanged. Slight oscillations can be seen in r channel and unwanted oscillations exist in Φ and Θ under H_∞ control, while the μ-synthesis controller delivered a stable performance consistently. The unwanted oscillations in signal-based H_∞ controller is mainly due to the increased model uncertainty. It can be clearly seen that both types of centralized controllers performed almost identically when the system uncertainties are low. This is evident in Fig. 11 to 13.

As the level of internal disturbance increased, the capabilities of the two control systems became evident. In particular, the signal-based H_∞ controller began to suffer under the increased system uncertainties, while the μ-synthesis controller remained functional reasonably well. The comparative results are shown in Fig. 14 to 16. The μ-synthesis method offers a robuster performance because it can explicitly take the uncertainty into account when designing the controller.

The proposed μ-controller is in state space form with 10 inputs, 4 outputs and 28 states, the implementation of such a controller on a modern ECU and its real-time performance are not of much concern thanks to powerful but common CPUs. As a result of the centralized structure, designers don't need to tune multi-loop controllers back and forth. Since the controller takes the helicopter as a complete system, it is capable to handle the coupling effect much better than those decentralized ones. According to the two tests in simulations, the controlled system behaves like

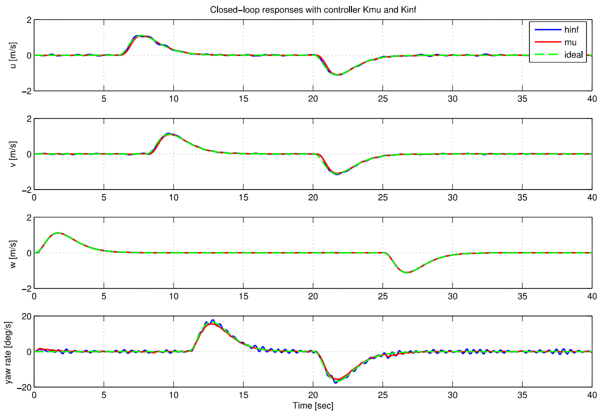

Fig. 14 Test 2 - Controlled velocities.

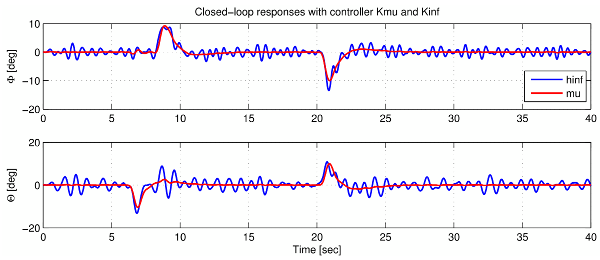

Fig. 15 Test 2 - Controlled roll and pitch.

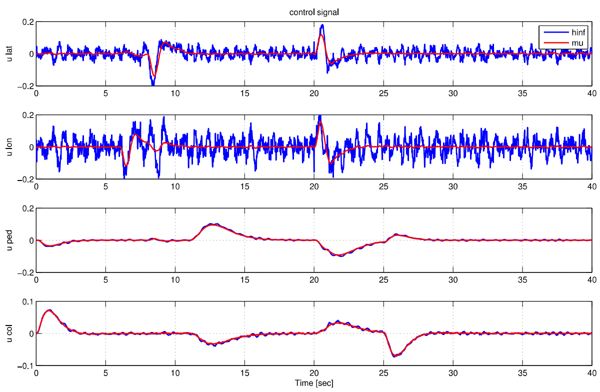

Fig. 16 Test 2 - Inputs to the four actuators.

four decoupled subsystems and the effect from other inputs to one channel is quite insignificant (Fig. 11 to 13). It's superior to those decentralized controllers in the literature[7, 10, 11]. When specific information and requirements of the system are available for the control design, the proposed controller would be more effective to use and much easier to tune than those decentralized ones.

5 Conclusion

The paper presented a very credible control design methodology, namely the μ-synthesis. The method was used to design a centralized controller to stabilize an unmanned helicopter, namely control the directional velocities u, v, w and the heading rate r. The novelty in the presentation of this paper is that, no partitioning of the LTI MIMO model has been made to design the controllers. The entire controller is designed by keeping the system model as a whole and hence has a higher level of performance in counter attacking coupling effects, un-modelled phenomena such as the system uncertainties as well as wind gusts and sensor noises. The μ-synthesis controller also has a greater capability to sustain in the presence of increased modelling uncertainty than the conventional robust controllers based on H_∞ theory. In the next step, the proposed controller will be further tested on our testbed.

References

[1] W. Yuan and J. Katupitiya, "A time-domain grey-box system identification procedure for scale-model helicopters," in *Proceedings of the 13th Australian Conference on Robotics and Automation*, Melbourne, Australia, 2011.

[2] ——, "A grey-box system identification procedure for scale-model helicopters based on frequency-domain estimation methods," in *Proceedings of the 28th Congress of the International Council of the Aeronautical Sciences*, Brisbane, Australia, September 2012.

[3] K. Peng, G. Cai, B. M. Chen, M. Dong, K. Y. Lum, and T. H. Lee, "Design and implementation of an autonomous flight control law for a uav helicopter," *Automatica*, vol. 45, no. 10, pp. 2333 – 2338, 2009.

[4] B. Mettler, M. Tischler, T. Kanade, and W. Messner, "Attitude control optimization for a small-scale unmanned helicopter," in *AIAA guidance, navigation and control conference*, 2000, pp. 40–59.

[5] D. H. Shim, H. J. Kim, and S. Sastry, "Control system design for rotorcraft-based unmanned

aerial vehicles using time-domain system identification," in *Proc. IEEE Int Control Applications Conf*, 2000, pp. 808–813.

[6] ——, "Decentralized nonlinear model predictive control of multiple flying robots," in *Proc. 42nd IEEE Conf. Decision and Control*, vol. 4, 2003, pp. 3621–3626.

[7] M. F. Weilenmann, U. Christen, and H. P. Geering, "Robust helicopter position control at hover," in *Proc. American Control Conf*, vol. 3, 1994, pp. 2491–2495.

[8] D. H. Shim, "Hierarchical flight control system synthesis for rotorcraft-based unmanned aerial vehicles," Ph.D. dissertation, UNIVERSITY OF CALIFORNIA, BERKELEY, 2000.

[9] R. Enns and J. Si, "Helicopter trimming and tracking control using direct neural dynamic programming," *IEEE Transactions on Neural Networks*, vol. 14, no. 4, pp. 929–939, 2003.

[10] B. Mettler, *Identification Modeling and Characteristics of Miniature Rotorcraft*. Kluwer Academic Publishers, 2003.

[11] M. La Civita, G. Papageorgiou, W. C. Messner, and T. Kanade, "Design and flight testing of an h-infinity controller for a robotic helicopter," *Journal of Guidance, Control, and Dynamics*, vol. 29, no. 2, pp. 485–494, March-April 2006.

[12] G. Cai, B. M. Chen, X. Dong, and T. H. Lee, "Design and implementation of a robust and nonlinear flight control system for an unmanned helicopter," *Mechatronics*, vol. 21, no. 5, pp. 803 – 820, 2011, special Issue on Development of Autonomous Unmanned Aerial Vehicles.

[13] S. Skogestad and I. Postlethwaite, *Multivariable feedback control analysis and design*, 2nd ed. Wiley, 2007.

[14] J. Gadewadikar, F. Lewis, K. Subbarao, K. Peng, and B. Chen, "H-infinity static output-feedback control for rotorcraft," *Journal of Intelligent & Robotic Systems*, vol. 54, pp. 629–646, 2009, 10.1007/s10846-008-9279-5.

[15] G. Balas, J. Doyle, K. Glover, A. Packard, and R. Smith, *μ-Analysis and Synthesis Toolbox: For Use with MATLAB, UserâĂŹs Guide, Version 3. The MathWorks*. Inc, 2001.

[16] B. Mettler, M. B. Tischler, and T. Kanade, "System identification of small-size unmanned helicopter dynamics," in *American Helicopter Society 55th Forum, Montreal, Quebec, Canada*, 1999.

[17] G. Balas, R. Chiang, A. Packard, and M. Safonov, *Robust Control Toolbox for Use with MATLAB*. The Math Works, Inc, 2006.

Copyright Statement